

# A novel CCU approach of CO<sub>2</sub> by the system 1,2-ethylenediamine+1,2-ethylene glycol

Bo Guo, Tianxiang Zhao, Feng Sha, Fei Zhang, Qiang Li, and Jianbin Zhang<sup>†</sup>

College of Chemical Engineering, Inner Mongolia University of Technology, Huhhot 010051, China

(Received 7 September 2015 • accepted 25 January 2016)

**Abstract**—As a new, effective CO<sub>2</sub> fixation system, 1,2-ethylenediamine and 1,2-ethylene glycol (EDA+EG) can efficiently activate CO<sub>2</sub> and directly convert it into a novel CO<sub>2</sub>-storage material (CO<sub>2</sub>SM) with 46.3% yield. The aqueous CO<sub>2</sub>SM solution can react with Ca(OH)<sub>2</sub>-saturated limpid solution to generate morphology-controllable CaCO<sub>3</sub> micro-particles with additional CO<sub>2</sub> bubbling and Ca(OH)<sub>2</sub>. Additionally, the aqueous EDA+EG solution could be recycled multiple times without significant loss of CO<sub>2</sub> capturing and releasing capabilities.

**Keywords:** CO<sub>2</sub> Capture, Storage and Utilization, CO<sub>2</sub>-storage Material, Absorption-desorption Cycle, CaCO<sub>3</sub> Micro-particle

## INTRODUCTION

In an effort to control the concentration of atmospheric carbon dioxide (CO<sub>2</sub>), a very important greenhouse gas produced by various industrial processes [1-5], the reduction, capture or utilization of CO<sub>2</sub> has become one of the greatest scientific and technological challenges in the 21st century [6-9]. CO<sub>2</sub> capture and storage/sequestration (CCS) [10-13] into adsorbents [14-17] has been mainly based on the adsorption [18] and membrane separation technology [19,20]. Compared with CCS, a CO<sub>2</sub> capture and utilization (CCU) approach [21] would be more attractive because it would not only consume thermodynamically stable CO<sub>2</sub> but also produce value-added chemicals [22-24]. For example, numerous systems based on liquid primary or secondary amines have been developed [25,26] to chemically convert CO<sub>2</sub> into carbamic acids and the corresponding ammonium carbamates. Then, dehydration of the generated ammonium carbamates could generate substituted ureas and the fixed CO<sub>2</sub> could be released upon heating. However, these processes have major drawbacks, such as a corrosive nature and volatility of the amines, their occasional decomposition and the high energy cost of their regeneration [27-32]. Jeesop et al. [33-36] reported an innovative class of CO<sub>2</sub> binding organic liquids (CO<sub>2</sub>BOLs), amidinium or guanidinium alkylcarbonate salts with good reactivity and high absorption capacity, which were generated from an alcohol and an amidine (or guanidine) superbase. Nevertheless, these systems are still expensive and are not able to attract significant industrial attention.

It has been known that 1,2-ethylenediamine (EDA) can react readily with CO<sub>2</sub> with an absorption ability of about 0.46 mol(CO<sub>2</sub>)/mol(EDA) [37]; however, the volatility of EDA significantly reduces its CO<sub>2</sub> absorption ability. Park et al. [38] reported that amidines could react efficiently with CO<sub>2</sub> to produce alkylcarbonate salts in the presence of an alcohol, and it was believed that the hydrogen bonding interactions and the hydrogen bonded structures in the

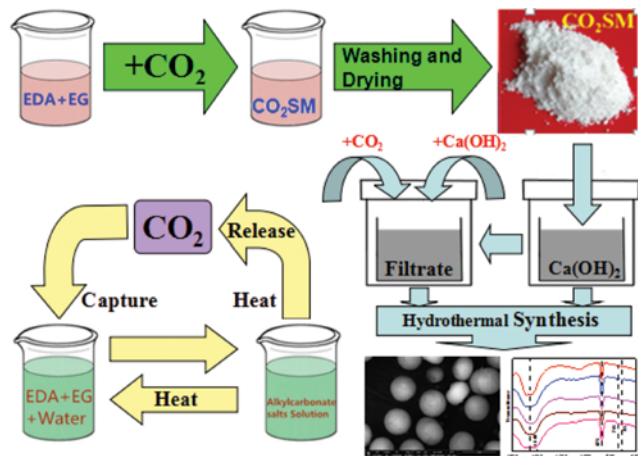


**Fig. 1.** A simplified process flow diagram of EDA+EG based CCU, the process by which the system EDA+EG was used to react with CO<sub>2</sub> under mild condition. A potential application of alkylcarbonate salts (CO<sub>2</sub>SM) would take advantage of release CO<sub>2</sub> of CO<sub>2</sub>SM as original materials to develop power CaCO<sub>3</sub> materials. And the aqueous EDA+EG solution was recycled multiple times to CO<sub>2</sub> capturing and releasing without any important loss of CO<sub>2</sub> capability.

amine-alcohol mixed solvents decreased the loss of amines [39,40].

In this study, an anhydrous system of EDA and EG (1 : 1 molar ratio) was developed to capture, store, and convert CO<sub>2</sub> into CO<sub>2</sub>SM at room temperature under atmospheric pressure, as shown in Fig. 1. The captured CO<sub>2</sub> could be released from the aqueous CO<sub>2</sub>SM solution to react with the Ca(OH)<sub>2</sub>-saturated limpid solution repeatedly, thus continuously producing CaCO<sub>3</sub> microparticles with controlled morphologies.

## MATERIALS AND METHODS

### 1. Materials

The analytical grade EG was purchased from Beijing Reagent

<sup>†</sup>To whom correspondence should be addressed.

E-mail: tadzhang@pku.edu.cn

Copyright by The Korean Institute of Chemical Engineers.

Company (Beijing, China, Content  $\geq 99.0\%$ ). The analytical grade EDA was purchased from Beijing Reagent Company (Beijing, China, Residue on ignition  $\leq 0.1\%$ ). They were used after drying over 0.4 nm molecular sieves and decompression filtration before measurements, and were degassed by ultrasound just before the experiments. The purity of final EG, as found by gas chromatograph (GC), was better than 99.3%. The compressed pure CO<sub>2</sub> (99.999% vol) gas was purchased from the Beijing Gas Company. Deionized water was used throughout the experiments. All other reagents used were analytical grade and were used without further purification.

## 2. Conversion of CO<sub>2</sub> into CO<sub>2</sub>SM

CO<sub>2</sub> was bubbled through approximately 40 g of the EDA+EG (1 : 1 mole ratio) solution continuously for about 90 min under mild conditions, and the weight, temperature, and electrical conductivity changes were recorded every minute. The electrical conductivity of solution was measured with a highly sensitive conductivity meter (DDSJ-308A) having a temperature accuracy of  $\pm 0.02$  K. The EDA+EG system was also used to capture CO<sub>2</sub> into solid CO<sub>2</sub>SM. The as-made CO<sub>2</sub>SM was washed with ethanol and dried under vacuum at 60 °C for 3 h. XRD measurements were carried out on a Siemens D/max-RB powder X-ray diffractometer with a 2θ range of 10–70°. FTIR spectra of solid samples were taken as 1% dispersion on a Nexus 670 FTIR spectrometer with a resolution of 1 cm<sup>-1</sup> in the range of 4,000–400 cm<sup>-1</sup>, and a base line correction was made for the spectra recorded in air at room temperature. <sup>13</sup>C-NMR spectrum was recorded on a Bruker ARX-400 nuclear magnetic resonance spectrometer with a 4 mm standard CP/MAS probe.

## 3. Properties and Utilization of CO<sub>2</sub>SM

For thermogravimetric analysis (TGA, Entzsch-Sta 449) of CO<sub>2</sub>SM, the sample was heated to 400 °C at a heating rate of 10 °C/min under a flow of nitrogen. For stability tests, CO<sub>2</sub>SM powder was made into tablets and then exposed to air and sunlight for 100 d. In addition, an aqueous CO<sub>2</sub>SM solution was reacted with a Ca(OH)<sub>2</sub>-saturated limpid solution at 100 °C for 1 h to afford CaCO<sub>3</sub> microparticles with controlled morphologies. The as-obtained CaCO<sub>3</sub> was washed with water and ethanol, and dried under vacuum at 120 °C for 5 h. The absorption-preparation cycles were carried out similarly, in which the aqueous CO<sub>2</sub>SM solution reacted with the Ca(OH)<sub>2</sub>-saturated limpid solution to afford CaCO<sub>3</sub> microparticles, and then the filtrate with EDA and EG but without CaCO<sub>3</sub> precipitate was reused to absorb CO<sub>2</sub>. After the adsorption of CO<sub>2</sub>, an appropriate amount of Ca(OH)<sub>2</sub> solution was added into the absorbent system to prepare the CaCO<sub>3</sub> precipitate again.

## 4. Absorption-desorption Processes

Absorption-desorption cycles of the aqueous EDA+EG system with CO<sub>2</sub> were at an absorption temperature of 20 °C and a desorption temperature of 97 °C under ambient pressure. The absorption process was conducted for 15 min and desorption for 90 min. All reactions were in a 100 mL gas-washing bottle, and the mass was measured on an electronic balance with an accuracy of 0.1 mg (Sartorius BS224S). Desorption experiments were carried out after the absorption. The CO<sub>2</sub>-saturated absorption system was heated in a pre-heated oil bath. The absorption-desorption cycle was continued after the system was cooled.

## RESULTS AND DISCUSSION

### 1. Mechanism Study of Absorbing CO<sub>2</sub>

Before the CO<sub>2</sub> absorption capability of the EDA+EG system was determined, the absorption of CO<sub>2</sub> in pure EDA or EG was studied under the same conditions. Results showed that the pure EDA reacted rapidly with bubbling CO<sub>2</sub> to become a viscous liquid. Because the reaction was exothermic, the solution temperature reached 100 °C. The maximum CO<sub>2</sub> absorption capability was about 0.46 mol(CO<sub>2</sub>)/mol(EDA). In contrast, the maximum CO<sub>2</sub> absorption capability in pure EG was about 0.0031 mol(CO<sub>2</sub>)/mol(EG), suggesting that EG had a very weak action on CO<sub>2</sub>. Additionally, no solid product was formed in either pure EDA or pure EG with bubbling CO<sub>2</sub>.

Although EDA could strongly absorb CO<sub>2</sub>, volatilization of EDA reduced its CO<sub>2</sub> absorption capabilities significantly. Because of the close intermolecular interactions formed when the molar ratio of EDA to EG was 1 : 1 [40], in this study, CO<sub>2</sub> absorption capability, temperature, and conductivity of the EDA+EG system with 1 : 1 molar ratio were recorded and shown in Fig. 2.

As shown in Fig. 2(a), weight of product was increased with increasing reaction time. The reaction was complete within about 20 min, and the maximum CO<sub>2</sub> absorption capacity reached about 0.79 mol(CO<sub>2</sub>)/mol(EDA), which was higher than that of various aqueous alkanolamines [41–43], including MEA (0.4628 mol CO<sub>2</sub> per mol amine), DEA (0.2360 mol CO<sub>2</sub> per mol amine), TEA (0.1944 mol CO<sub>2</sub> per mol amine), DGA (0.7796 mol CO<sub>2</sub> per mol amine), and MDEA (1.3442 mol CO<sub>2</sub> per mol amine). The temperature change of the solution (Fig. 2(b)) showed that the process was exothermic and that the system reached its maximum temperature within about 20 min. After the reaction was finished and the temperature had reached its highest point, the temperature dropped upon the formation of dope, which attenuated the mass transfer of the system. As shown in Fig. 2(c), the initial conductivity of the anhydrous EDA+EG system was 32.8 μS/cm. When the CO<sub>2</sub> was bubbled, its conductivity was increased rapidly as an ionic com-

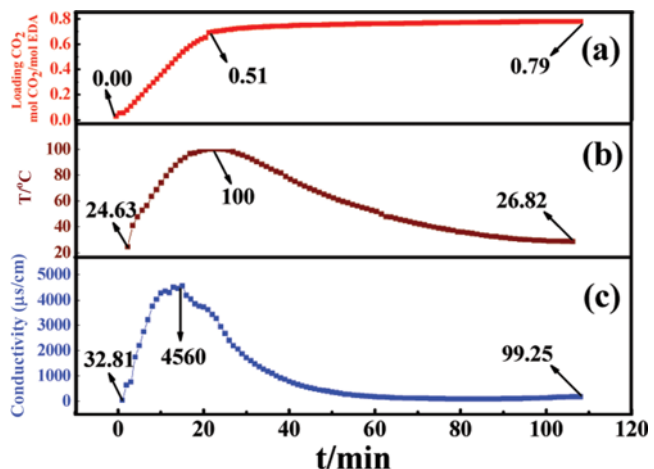


Fig. 2. The variation of weight (a), temperature (b), and electrical conductivity (c) changes for EDA+EG system at CO<sub>2</sub> flow rate of 250 ml/min.

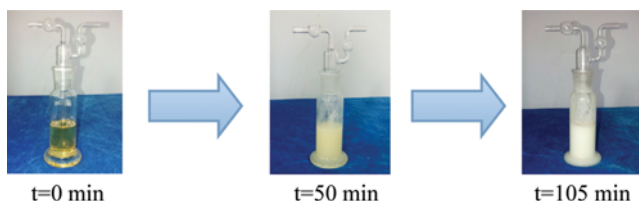


Fig. 3. The reaction process of EDA+EG with CO<sub>2</sub> at various time.

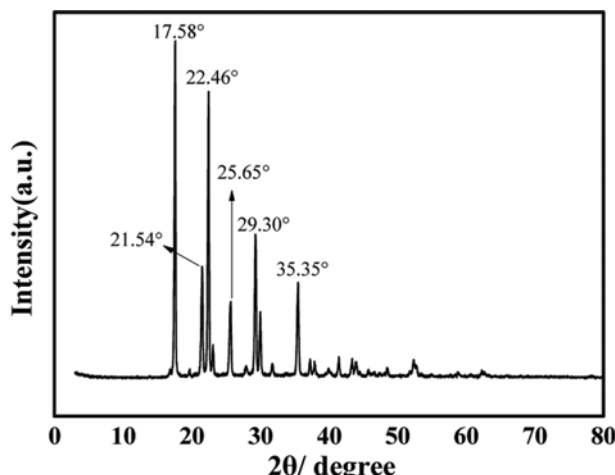


Fig. 4. XRD spectrum of CO<sub>2</sub>SM.

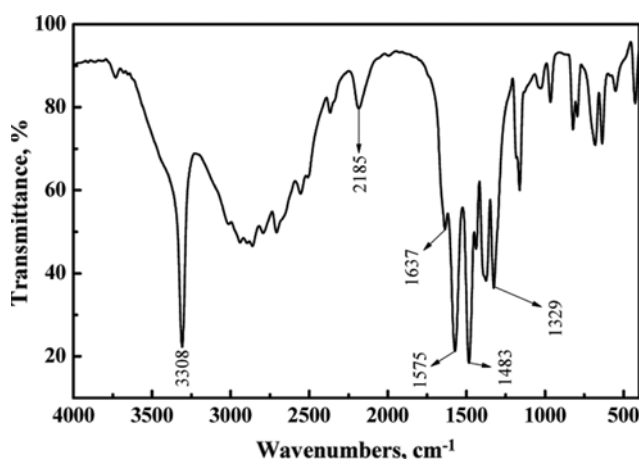


Fig. 5. FTIR spectrum of CO<sub>2</sub>SM.

ound was formed. The maximum conductivity was about 4,560  $\mu\text{S}/\text{cm}$ . Nevertheless, with the longer reaction times, the solution became more and more viscous, and as ion movement was hindered, the conductivity was decreased. In both cases, the reaction system appeared cloudy at the end of the reaction due to the formation of a fine suspension of a white solid CO<sub>2</sub>SM as shown in

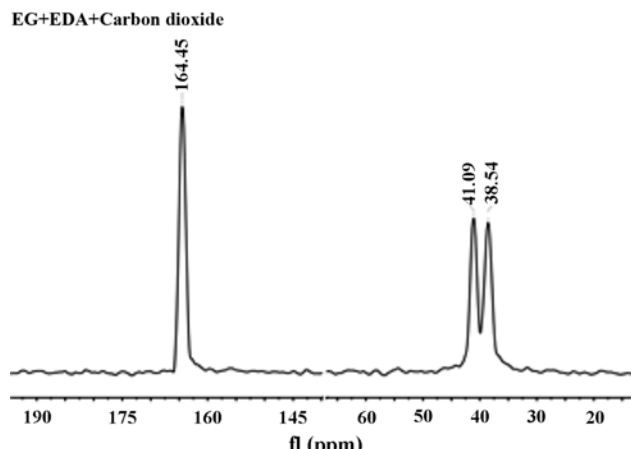


Fig. 6.  $^{13}\text{C}$ -NMR spectrum of CO<sub>2</sub>SM.

Fig. 3.

The as-made CO<sub>2</sub>SM was washed three times with ethanol and dried for 3 h. The dried CO<sub>2</sub>SM was characterized with XRD (Fig. 4), FTIR (Fig. 5) and  $^{13}\text{C}$ -NMR (Fig. 6). The XRD pattern showed that CO<sub>2</sub>SM had characteristic peaks at 17.58°, 21.54°, 22.46°, 25.65°, 29.30° and 35.35°, which is similar to the peak pattern found with ethylenediamine carbamate ( $-\text{NH}-\text{CO}_2^-$ ) characteristic diffraction peaks.

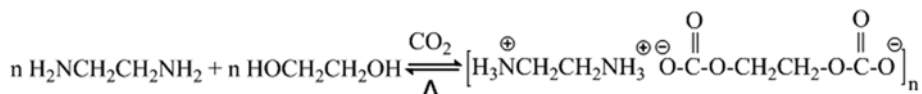
As shown in Fig. 5, the peak at 3,308  $\text{cm}^{-1}$  was assigned to the stretching vibration of N-H [44,45] and characteristic peak of primary ammonium salts ( $\text{NH}_3^+$ ) was found at 2,185  $\text{cm}^{-1}$  [21]. The peak at 1,637  $\text{cm}^{-1}$  was assigned to the deformation of  $\text{NH}_3^+$  [46], 1,575  $\text{cm}^{-1}$  and 1,483  $\text{cm}^{-1}$  were attributed to  $-\text{CO}_2^-$  asymmetric and symmetric stretching vibrations [47-50] and 1,329  $\text{cm}^{-1}$  was assigned to N-CO<sub>2</sub><sup>-</sup> skeletal vibrations [46]. However, the out-of-plane vibration of bicarbonate anion appeared at 835  $\text{cm}^{-1}$  [51,52]. Therefore, the as-obtained solid product was likely composed of alkylcarbonate salts.

To further determine the alkylcarbonate salt rather than the bicarbonate [53], a  $^{13}\text{C}$ -NMR spectrum of the solid CO<sub>2</sub>SM was obtained as shown in Fig. 6.

The new peak at 164.45 ppm was consistent with an alkylcarbonate salt [54,55] because the bicarbonate anion is often found at 160.4 ppm [51]. Peaks at 41.09 and 38.54 ppm were assigned to the  $-\text{CH}_2-$  [49]. Therefore, according to these results and our previous work [40], a possible formation mechanism of CO<sub>2</sub>SM was proposed (Scheme 1). Similarly, Jessop et al. [33-36,56] also presented a class of CO<sub>2</sub> binding organic liquids (CO<sub>2</sub>BOL) which produced amidine or guanidine alkylcarbonate salts from an alcohol and an amidine or guanidine superbase.

## 2. Characteristic and Utilization of CO<sub>2</sub>SM

As shown in Fig. 7, a TGA of CO<sub>2</sub>SM, the decomposition of CO<sub>2</sub>SM began approximately at 60 °C with small quantities of CO<sub>2</sub>



Scheme 1. EDA+EG system react with CO<sub>2</sub> give to alkylcarbonate salt.

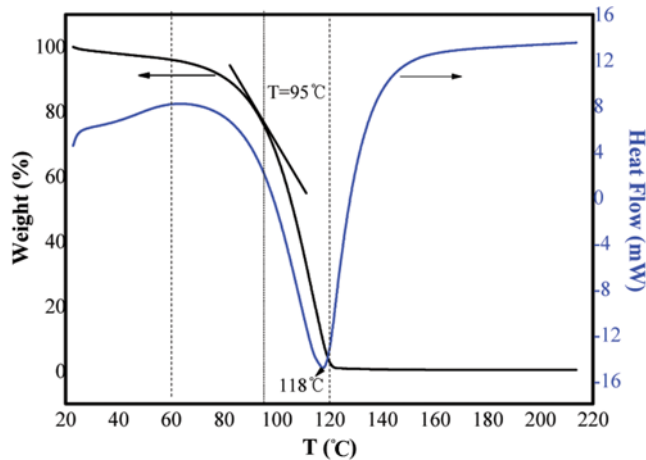


Fig. 7. Thermogravimetric analysis curves of  $\text{CO}_2\text{SM}$ .

and EDA released. Decomposition accelerated at about  $95^\circ\text{C}$  with more  $\text{CO}_2$  released. At about  $118^\circ\text{C}$ , a large exothermic peak was observed because the thermal decomposition of EDA and the release of  $\text{CO}_2$  were completed.

Additionally, when the  $\text{CO}_2\text{SM}$  powder was made into tablets and exposed to air and sunlight for 100 d,  $\text{CO}_2\text{SM}$  was found to be stable (Fig. S1).

### 3. Preparation of $\text{CaCO}_3$

Based on the TGA result,  $\text{CO}_2\text{SM}$  could release  $\text{CO}_2$  at  $100^\circ\text{C}$ . The  $\text{CO}_2$  released from the aqueous  $\text{CO}_2\text{SM}$  solution could then react with the  $\text{Ca}(\text{OH})_2$ -saturated limpid solution to generate  $\text{CaCO}_3$  microparticles via hydrothermal synthesis at  $100^\circ\text{C}$  within 1 h. Most importantly, the as-released EDA and EG from those processes could act as surfactants. Therefore, the as-made  $\text{CaCO}_3$  morphology could be controlled by adjusting the  $\text{CO}_2\text{SM}$  concentration. For example, belt shaped product was obtained using  $0.6 \text{ g}\cdot\text{L}^{-1}$  of  $\text{CO}_2\text{SM}$ , while spherical shaped was obtained using  $60 \text{ g}\cdot\text{L}^{-1}$  of  $\text{CO}_2\text{SM}$  (Figs. 8 and 9). These results indicated that there were different phases of  $\text{CaCO}_3$  under different concentrations of  $\text{CO}_2\text{SM}$ . Furthermore, the filtrate containing EDA and EG without  $\text{CaCO}_3$  precipitate could be reused to absorb  $\text{CO}_2$ . After the adsorption of  $\text{CO}_2$ ,  $\text{CaCO}_3$  precipitate was formed with an appropriate amount of  $\text{Ca}(\text{OH})_2$  solution added into the absorbent system.  $\text{CaCO}_3$  microspheres still could be produced smoothly at  $100^\circ\text{C}$  within

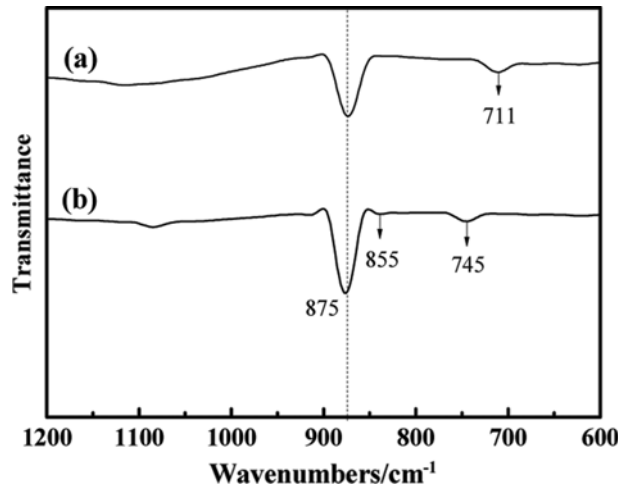


Fig. 9. FTIR spectra of morphologies  $\text{CaCO}_3$  material from the reaction of  $\text{CO}_2\text{SM}$  with  $\text{Ca}(\text{OH})_2$  via hydrothermal synthesis at  $100^\circ\text{C}$  for 1 h, in which the concentration of  $\text{CO}_2\text{SM}$  were  $0.6 \text{ g}\cdot\text{L}^{-1}$  (a) and  $60 \text{ g}\cdot\text{L}^{-1}$  (b), respectively.

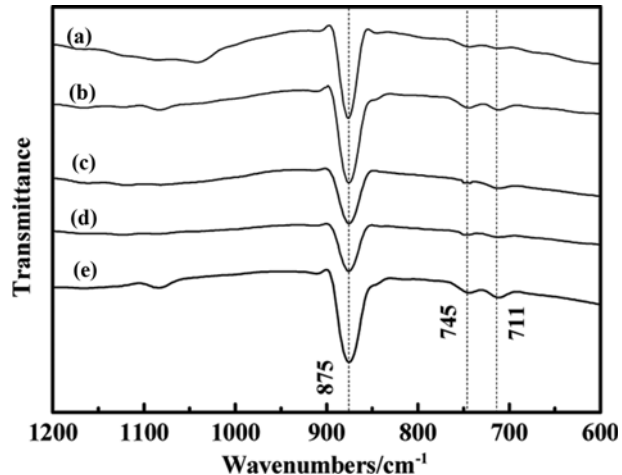


Fig. 10. FTIR spectra of the circular preparation of  $\text{CaCO}_3$  microspheres. (a)-(e) represents the number of experiments.

1 h after five-successive absorption-preparation cycles. FTIR results (Fig. 10) showed that all  $\text{CaCO}_3$  particles had the same phase. These results showed that the filtered solution without  $\text{CaCO}_3$  pre-

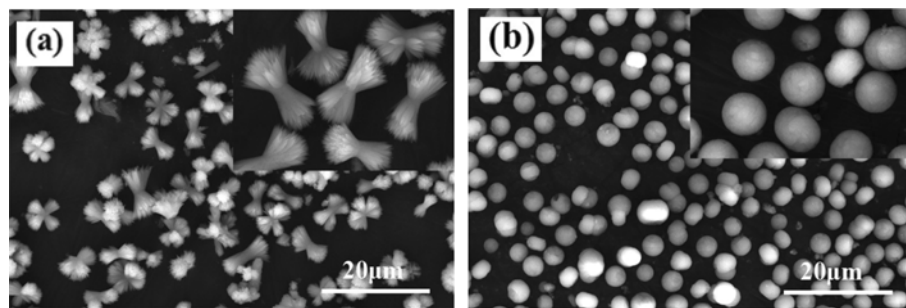
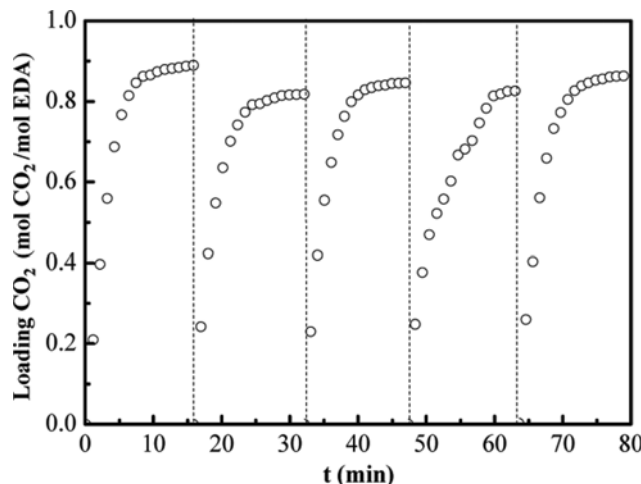


Fig. 8. SEM images of morphologies  $\text{CaCO}_3$  material from the reaction of  $\text{CO}_2\text{SM}$  with  $\text{Ca}(\text{OH})_2$  via hydrothermal synthesis at  $100^\circ\text{C}$  for 1 h, in which the concentration of  $\text{CO}_2\text{SM}$  were  $0.6 \text{ g}\cdot\text{L}^{-1}$  (a) and  $60 \text{ g}\cdot\text{L}^{-1}$  (b), respectively.



**Fig. 11.** Reversible CO<sub>2</sub> capture and release by the 15 wt% aqueous EDA+EG system, where capture was performed at 20 °C and atmospheric pressure with a CO<sub>2</sub> flow rate of 250 ml/min and release at 97 °C with stirring.

cipitate could not only be used to absorb CO<sub>2</sub> repeatedly, but also to produce CaCO<sub>3</sub> microspheres repeatedly after the additional bubbling of CO<sub>2</sub> into the aqueous CO<sub>2</sub>SM solution.

#### 4. Absorption-desorption Cycles

Typically, CO<sub>2</sub> absorption with the aqueous EDA+EG (molar ratio 1:1) system was conducted at 20 °C under an atmospheric pressure and sample weight changes were recorded with an electronic balance. According to the TGA curve (Fig. 7), desorption of CO<sub>2</sub> from the loaded solution was carried out at 97 °C with stirring until no CO<sub>2</sub> was released from the solution, which lasted for 90 min. The continuous cycling of CO<sub>2</sub> absorption-desorption was as shown in Fig. 11.

As shown in Fig. 11, the aqueous EDA+EG solution could be recycled at least for five continuous absorption-desorption cycles without any significant loss of CO<sub>2</sub> capturing and releasing capability. The regeneration temperature, lower than that of the traditional MEA system, was in the range of 100–140 °C [57], probably due to the much lower thermostability of the formed alkylcarbonate salts. The maximum CO<sub>2</sub> loading capacity reached 1.2602 mol (CO<sub>2</sub>)/mol(EDA) [41–43] in the absorption-desorption cycles. Therefore, the aqueous EDA+EG (molar ratio 1:1) system could provide high loading capacity, stable absorption-desorption cycles, and low energy requirements for the industry to not only attenuate the volatilization of EDA, but also to capture and utilize CO<sub>2</sub> with limited energy loss.

#### CONCLUSION

The anhydrous EDA+EG system can absorb CO<sub>2</sub> under mild conditions to form the novel solid CO<sub>2</sub>SM by alkylcarbonate chemical binding, in which EG could successfully fix EDA to significantly decrease the loss of EDA due to volatilization. The aqueous CO<sub>2</sub>SM solution can react with the Ca(OH)<sub>2</sub>-saturated limpid solution to generate CaCO<sub>3</sub> microparticles with controllable morphologies. Additionally, the aqueous EDA+EG solution can have strong

CO<sub>2</sub> absorption capability after multiple cycles of absorption (20 °C under an atmospheric pressure) and desorption (97 °C with stirring).

#### ACKNOWLEDGEMENTS

This work was supported by the National Natural Science Foundation of China (21166017), the Research Fund for the Doctoral Program of Higher Education of China (20111514120002), the Inner Mongolia Science and Technology Key Projects, the Program for Grassland Excellent Talents of Inner Mongolia Autonomous Region, Program for New Century Excellent Talents in University (NCET-12-1017), and the Inner Mongolia Talented People Development Fund.

#### SUPPORTING INFORMATION

Additional information as noted in the text. This information is available via the Internet at <http://www.springer.com/chemistry/journal/11814>.

#### REFERENCES

- P. Mores, N. Scenna and S. Mussati, *Energy*, **45**, 1042 (2012).
- K. Han, C. K. Ahn, M. S. Lee, C. H. Rhee, J. Y. Kim and H. D. Chun, *Int. J. Greenh. Gas Con.*, **14**, 270 (2013).
- F. F. Li, Z. H. Yang, R. Zeng, G. Yang, X. Chang, J. B. Yan and Y. L. Hou *Ind. Eng. Chem. Res.*, **50**, 6496 (2011).
- M. Zaman and J. H. Lee, *Korean J. Chem. Eng.*, **30**, 1497 (2013).
- S. C. Ma, G. D. Chen, T. T. Han, S. J. Zhu and J. Yang, *Int. J. Greenh. Gas Con.*, **37**, 249 (2015).
- R. Carapellucci, L. Giordano and M. Vaccarelli, *Energy*, **85**, 594 (2015).
- A. Goeppert, M. Czaun, G. K. S. Prakash and G. A. Olah, *Energy Environ. Sci.*, **5**, 7833 (2012).
- A. J. Hunt, E. H. K. Sin, R. Marriott and J. H. Clark, *ChemSusChem*, **3**, 306 (2010).
- V. Barbarossa, F. Barzaghi, F. Mani, S. Lai, P. Stoppioni and G. Vanga, *RSC Adv.*, **3**, 12349 (2013).
- R. Sathre, M. Chester, J. Cain and E. Masanet, *Energy*, **37**, 540 (2012).
- H. Li, M. Ditaranto and D. Berstad, *Energy*, **36**, 1124 (2011).
- H. Jin, L. Gao, W. Han and H. Hong, *Energy*, **35**, 4499 (2010).
- J. P. Sculley and H. C. Zhou, *Angew. Chem. Int. Ed.*, **51**, 12660 (2012).
- D. Bonenfant, M. Mimeault and R. Hausle, *Ind. Eng. Chem. Res.*, **42**, 3179 (2003).
- D. Camper, J. E. Bara and D. L. Gin, *Ind. Eng. Chem. Res.*, **47**, 8496 (2008).
- H. Seo, D. Y. Min, N. Y. Kang, W. C. Choi, S. Park, Y. Park and D. K. Lee, *Korean J. Chem. Eng.*, **32**, 51 (2015).
- T. Wang and K. Jens, *Int. J. Greenh. Gas Con.*, **37**, 354 (2015).
- J. Y. Wang, L. Huang, R. Y. Yang, Z. Zhang, J. W. Wu, Y. S. Gao, Q. Wang, D. O. Hare and Z. Y. Zhong, *Energy Environ. Sci.*, **7**, 3478 (2014).
- M. T. Ho, G. W. Allinson and D. E. Wiley, *Ind. Eng. Chem. Res.*, **47**, 1562 (2008).

20. J. Huang, J. Zou and W. S. Winston, *Ind. Eng. Chem. Res.*, **47**, 1261 (2008).
21. D. J. Heldebrant, P. K. Koech, T. M. Ang, L. Chen, J. E. Rainbolt, C. R. Yonkera and P. G. Jessop, *Green Chem.*, **12**, 713 (2010).
22. M. D'Alessandro, B. Smit and J. R. Long, *Angew. Chem. Int. Ed.*, **49**, 6058 (2010).
23. W. Jones and E. J. Maginn, *ChemSusChem.*, **3**, 863 (2010).
24. Y. Takeda, S. Okumura, I. Sasaki and S. Minakata, *Org Lett.*, **14**, 4874 (2012).
25. S. Kim, J. Kang, J. Lee and B. Min, *Korean J. Chem. Eng.*, **28**, 2275 (2011).
26. H. Lepaumier, D. Picq and P. L. Carrette, *Ind. Eng. Chem. Res.*, **48**, 9061 (2009).
27. G. S. Goff and G. T. Rochelle, *Ind. Eng. Chem. Res.*, **45**, 2513 (2006).
28. C. Gouedard, D. Picq, F. Launay and P. L. Carrette, *Int. J. Greenh. Gas Con.*, **10**, 244 (2012).
29. M. Karl, R. F. Wright, T. F. Berglen and B. Denby, *Int. J. Greenh. Gas Con.*, **5**, 439 (2011).
30. F. Mani, M. Peruzzini and P. Stoppioni, *Green Chem.*, **8**, 995 (2006).
31. K. Veltman, B. Sing and E. G. Hertwich, *Environ. Sci. Technol.*, **44**, 1496 (2010).
32. C. Zheng, J. Tan, Y. J. Wang and G. S. Luo, *Ind. Eng. Chem. Res.*, **51**, 11236 (2012).
33. P. G. Jessop, D. J. Heldebrant, X. Li, C. A. Eckert and C. L. Liotta, *Nature*, **436**, 1102 (2005).
34. X. Su, M. F. Cunningham and P. G. Jessop, *Chem. Commun.*, **49**, 2655 (2013).
35. X. Su, T. Robert, S. M. Mercer, C. Humphries, M. F. Cunningham and P. G. Jessop, *Chem. Eur. J.*, **19**, 5595 (2013).
36. P. G. Jessop, L. Phan, A. Carrier, S. Robinson, C. J. Durr and J. R. Harjani, *Green Chem.*, **12**, 809 (2010).
37. Y. Liu, P. G. Jessop, M. F. Cunningham, C. A. Eckert and C. L. Liotta, *Science*, **313**, 958 (2006).
38. M. Kim and J. Park, *Chem. Commun.*, **46**, 2507 (2010).
39. R. J. Sengwa, K. Klimaszewski and A. Borun, *J. Chem. Eng. Data*, **57**, 3164 (2012).
40. C. P. Li, J. B. Zhang, T. Zhang, X. H. Wei, E. Zhang, N. Yang, N. N. Zhao and M. Su, *J. Chem. Eng. Data*, **55**, 4104 (2010).
41. U. Maheswari and K. Palanivelu, *J. CO<sub>2</sub> Utilization*, **6**, 45 (2014).
42. J. Li, C. You, L. Chen, Y. Ye, Z. Qi and K. Sundmacher, *Ind. Eng. Chem. Res.*, **51**, 12081 (2012).
43. J. Li, L. Chen, Y. Ye and Z. Qi, *J. Chem. Eng. Data*, **59**, 1781 (2014).
44. J. P. Shang, S. M. Liu, X. Y. Ma, L. J. Lu and Y. Q. Deng, *Green Chem.*, **14**, 2899 (2012).
45. H. B. Wang, P. G. Jessop and G. J. Liu, *ACS Macro Lett.*, **1**, 944 (2012).
46. C. S. Srikanth and S. S. C. Chuang, *J. Phys. Chem. C*, **117**, 9196 (2013).
47. V. Blasucci, C. Dilek, H. Huttenhower, E. John, V. Llopis-Mestre, P. Pollet, C. A. Eckert and C. L. Liotta, *Chem. Commun.*, 116 (2009).
48. A. Danon, P. C. Stair and E. Weitz, *J. Phys. Chem. C*, **115**, 11540 (2011).
49. A. Dibenedetto, M. Aresta, C. Fragale and M. Narracci, *Green Chem.*, **4**, 439 (2002).
50. L. Phan, J. R. Andreatta, L. K. Horvey, C. F. Edie, A. L. Luco, A. Mirchandani, D. J. Darenbourg and P. G. Jessop, *J. Org. Chem.*, **73**, 127 (2008).
51. D. J. Heldebrant, P. G. Jessop, C. A. Thomas, C. A. Eckert and C. L. Liotta, *J. Org. Chem.*, **70**, 5335 (2005).
52. L. M. Scott, T. Robert, J. R. Harjani and P. G. Jessop, *RSC Adv.*, **2**, 4925 (2012).
53. A. N. M. Peeters, A. P. C. Faaij and W. C. Turkenburg, *Int. J. Greenh. Gas Con.*, **1**, 396 (2007).
54. F. Barzaghi, F. Mani and M. Peruzzini, *Energy Environ. Sci.*, **2**, 322 (2009).
55. A. Enrico, P. D. Eoghan, C. Laurie, B. A. Lawrence and R. B. Andrew, *Sci. Rep.*, **4**, 7304 (2014).
56. D. J. Heldebrant, C. R. Yonker, P. G. Jessop and L. Phan, *Energy Environ. Sci.*, **1**, 487 (2008).
57. M. Packer, *Energy Policy*, **37**, 3428 (2009).